Neural Evidence of Functional Compensation for Fluid Intelligence in Healthy Ageing

Authors: Ethan Knights [1], Richard N. Henson [1, 2], Alexa M. Morcom [3], Daniel J. Mitchell[1] & Kamen A. Tsvetanov [4, 5]

1 Medical Research Council Cognition and Brain Sciences Unit, United Kingdom.
2 Department of Psychiatry, University of Cambridge, United Kingdom.
3 School of Psychology, University of Sussex, Brighton, United Kingdom.
4 Department of Psychology, University of Cambridge, United Kingdom.
5 Department of Clinical Neurosciences, University of Cambridge, United Kingdom.

Corresponding Author: Kamen Tsvetanov, kat35@cam.ac.uk

Conflict of interest: The authors declare no competing financial interests.

Acknowledgments: For the purpose of open access, the author has applied a Creative Commons Attribution (CC BY) licence to any Author Accepted Manuscript version arising from this submission. The Cambridge Centre for Ageing and Neuroscience (Cam-CAN) research was supported by the Biotechnology and Biological Sciences Research Council (Grant No. BB/H008217/1). The project has also received funding from the European Union's Horizon 2020 research and innovation programme ('LifeBrain', Grant Agreement No. 732592), which supported E.K.; K.A.T. was supported by the Guarantors of Brain (G101149) and Alzheimer's Society (Grant No. 602). Corporate Cam-CAN authorship membership includes: Project principal personnel: Lorraine K Tyler, Carol Brayne, Edward T Bullmore, Andrew C Calder, Rhodri Cusack, Tim Dalgleish, John Duncan, Richard N Henson, Fiona E Matthews, William D Marslen-Wilson, James B Rowe, Meredith A Shafto; Research Associates: Karen Campbell, Teresa Cheung, Simon Davis, Linda Geerligs, Rogier Kievit, Anna McCarrey, Abdur Mustafa, Darren Price, David Samu, Jason R Taylor, Matthias Treder, Kamen A Tsvetanov, Janna van Belle, Nitin Williams, Daniel Mitchell, Ethan Knights; Research Assistants: Lauren Bates, Tina Emery, Sharon Erzinçlioglu, Andrew Gadie, Sofia Gerbase, Stanimira Georgieva, Claire Hanley, Beth Parkin, David Troy; Affiliated Personnel: Tibor Auer, Marta Correia, Lu Gao, Emma Green, Rafael Henriques; Research Interviewers: Jodie Allen, Gillian Amery, Liana Amunts, Anne Barcroft, Amanda Castle, Cheryl Dias, Jonathan Dowrick, Melissa Fair, Hayley Fisher, Anna Goulding, Adarsh Grewal, Geoff Hale, Andrew Hilton, Frances Johnson, Patricia Johnston, Thea Kavanagh-Williamson, Magdalena Kwasniewska, Alison McMinn, Kim Norman, Jessica Penrose, Fiona Roby, Diane Rowland, John Sargeant, Maggie Squire, Beth Stevens, Aldabra Stoddart, Cheryl Stone, Tracy Thompson, Ozlem Yazlik; and administrative staff: Dan Barnes, Marie Dixon, Jaya Hillman, Joanne Mitchell, Laura Villis.

Abstract

Functional compensation is a common notion in the neuroscience of healthy ageing, whereby older adults are proposed to recruit additional brain activity to compensate for reduced cognitive function. However, whether this additional brain activity in older participants actually helps their cognitive performance remains debated. We examined brain activity and cognitive performance in a human lifespan sample (N=223) while they performed a problem-solving task (based on Cattell's test of fluid intelligence) during functional magnetic resonance imaging (fMRI). Whole-brain univariate analysis revealed that activity in bilateral cuneal cortex for hard vs. easy problems increased both with age and with performance, even when adjusting for an estimate of age-related differences in cerebrovascular reactivity. Multivariate Bayesian decoding further demonstrated that age increased the likelihood that activation patterns in this cuneal region provided non-redundant information about the two task conditions, beyond that of the multiple-demand network generally activated in this task. This constitutes some of the strongest evidence yet for functional compensation in healthy ageing, at least in this brain region during visual problem-solving.

Introduction

Preventing cognitive decline in old age is a major public heath priority, which demands a better understanding of the neurophysiological changes that preserve cognitive function despite progressive brain atrophy (Cabeza et al., 2018; Christensen et al., 2009). Neuroimaging has facilitated the idea that the brain can flexibly respond to tissue loss (e.g., due to ageing) by recruiting additional brain activity to support cognitive functions (Cabeza et al., 2018; Grady, 2012). If this additional recruitment in older adults improves their behavioural performance, it is argued that this reorganisation of brain function constitutes a functional compensation mechanism (Cabeza, 2002).

Fluid intelligence (i.e., solving novel abstract problems) is a cognitive function that shows one of the most consistent and largest decreases in older age (Salthouse et al., 2008; Deary, 2012; Ghisletta et al., 2012; Kievit et al., 2014; Bors & Forrin, 1995; Salthouse & Pink, 2008; Schretlen et al., 2000; Clay et al., 2009; Kievit et al., 2018). Functional (Duncan et al., 2000; Gray et al., 2003; Lee et al., 2006; Crittenden et al., 2016; Tschentscher et al., 2017) and structural (Colom et al., 2009; Jauk et al., 2015; Chen et al. 2020; Paul et al., 2016; Zamroziewicz et al., 2018) neuroimaging has shown that fluid intelligence tasks engage the multiple demand network (MDN; Duncan, 2010), which comprises lateral prefrontal, posterior parietal and cingulate regions. MDN activation tends to decrease with age as measured, for example, with fMRI during problem-solving tasks that tax fluid intelligence such as the Cattell task (Samu et al., 2017; Mitchell et al., 2022). So far, these studies have examined age effects in core regions of the MDN but have not explicitly tested for functional compensation in other regions.

To search for brain regions that might support functional compensation, we conducted a whole-brain voxel-wise search for clusters that showed a positive relationship with both age and cognitive performance (i.e., classic univariate criteria for functional compensation; Lövdén et al., 2010; Cabeza et al., 2018). The dependent variable was the difference in fMRI activation for blocks of hard vs. easy odd-one-out problems (Figure 1A), as measured in 223 adults between 19 and 87 years of age, from Stage 3 of the Cambridge Centre for Ageing & Neuroscience (Cam-CAN) project (Shafto et al., 2014); performance was measured as the proportion of all problems correct. Second, we applied a Multi-Variate Bayesian approach (MVB; Friston et al., 2008) across all voxels within any candidate regions identified in the whole-brain search, to test whether multivoxel patterns in these regions provided additional information about task difficulty, beyond that in the MDN. We predicted that, if a region were involved in functional compensation, the additional information it contains about the task would increase with age. To pre-empt the results, unlike in our previous applications of MVB (Morcom & Henson, 2018; Knights et al., 2021), we find one region - within the cuneus - that did show evidence of this additional multivariate information, supporting its role in functional compensation.

Results

Behavioural Performance

As expected from prior studies, behavioural performance decreased with age during the fMRI scan on the modified version of the Cattell task (collapsed across hard and easy conditions; see Methods) (standardised coefficient = -5.65, $t(220) = -14$, $p < .001$, $R^2 = 0.48$; Figure 1B upper). There was a high correlation between

performance measures from the fMRI version and standard version of the Cattell task when the same people performed the standard Cattell task outside the scanner 1-3 years previously ($r = 0.79$, $p < 0.001$; Figure 1B lower), suggesting that the version modified for fMRI was capturing the same cognitive ability.

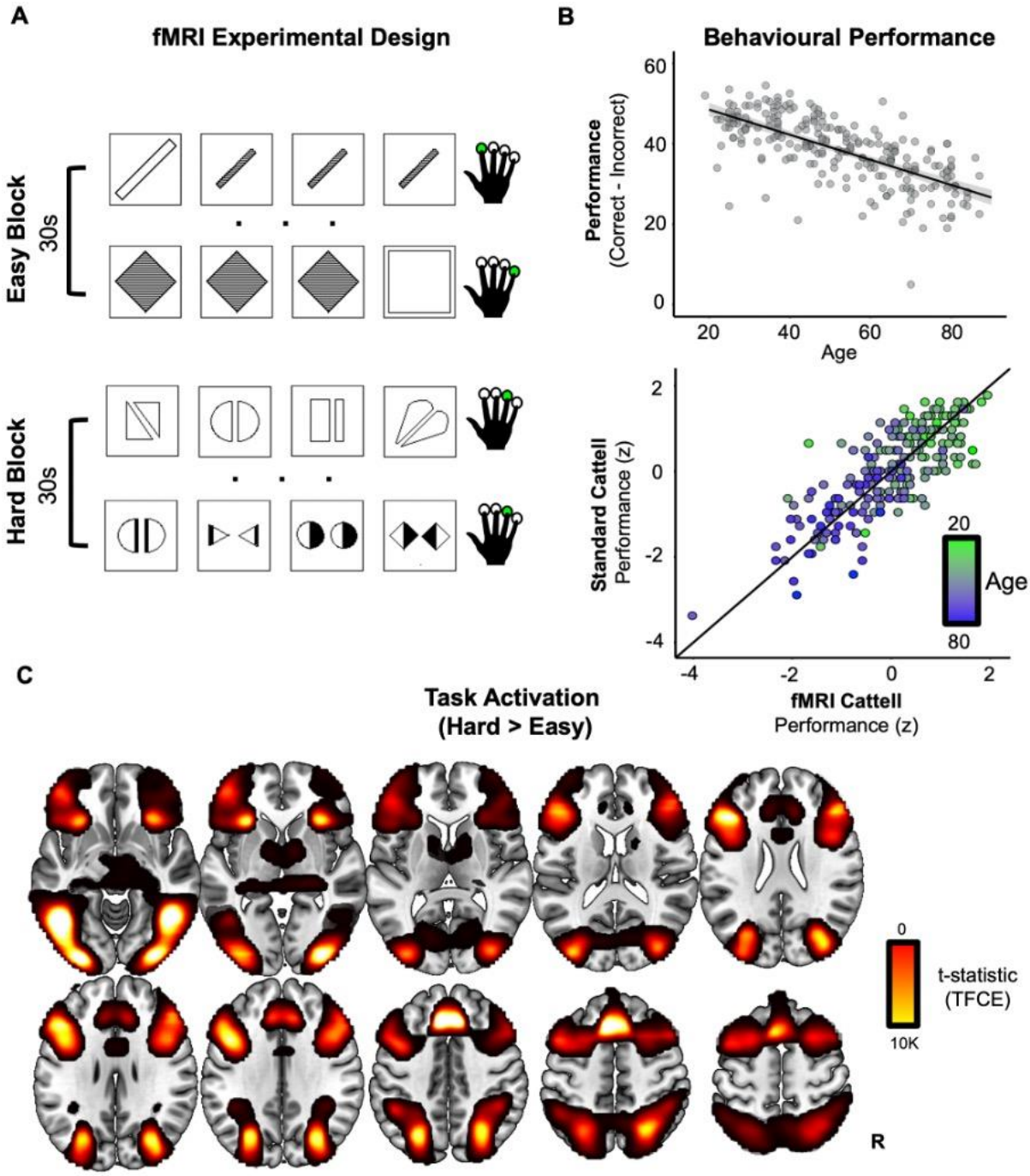

Figure 1. **(A) fMRI version of Cattell task.** On each trial (each row), participants select the odd-one-out from four panels with a single finger button-press (green circles). Condition blocks (30 seconds) alternate between easy vs. hard puzzles. **(B) Behavioural age-related decline.** Performance (correct minus incorrect in fMRI version of Cattell task) significantly declined linearly with age (upper). High reliability was observed between performance measures from the standard Cattell task and

the modified version used for fMRI (lower). In the upper panel, the black line represents the fitted-regression estimates with shaded 95% confidence intervals. In the lower panel, the black line represents perfect correlation between the two Cattell versions. **(C) Univariate task effect.** Whole-brain voxel-wise activations for solving the puzzles in the hard, relative to easy, blocks, after threshold-free cluster enhanced (TFCE) correction.

Univariate Response

The [Hard > Easy] contrast showed bilateral activation across regions generally described as comprising the MDN (e.g., Duncan 2010; Smith et al., 2021), including the inferior/middle frontal gyri, intraparietal sulcus, anterior insula and anterior cingulate cortex (Figure 1C). Additional activation was observed bilaterally in the inferior/ventral and lateral occipital temporal cortex, likely due to the visual nature of the task.

To search for a potentially compensatory pattern of brain activation, we next overlaid maps that tested for positive effects of age (Figure 2A green map) and performance (Figure 2A red map) on the [Hard > Easy] contrast. While age and performance are negatively correlated (Figure 1B), their effects were estimated simultaneously via multiple regression, and so the activation maps reflect unique effects of each. As reported using related measures and overlapping samples of Cam-CAN participants (Samu et al., 2017; Wu et al., 2021; Mitchell et al., 2022), age-related increases in activity were widespread, including the precuneus, middle frontal gyrus and supplementary motor area. Activity positively related to performance was found in many of the same regions that were more active for hard

versus easy problems (i.e., inferior/middle frontal gyrus, anterior cingulate, superior parietal lobule; Figure 1C).

Crucially, two areas of the brain showed spatially-overlapping positive effects of age and performance, which is suggestive of an age-related compensatory response (Figure 2A yellow intersection). These were in bilateral cuneal cortex (Figure 2B magenta) and bilateral frontal cortex (Figure 2B brown), the latter incorporating parts of the middle frontal gyri and anterior cingulate. Therefore, based on traditional univariate analyses, these are two candidate regions for age-related functional compensation (Cabeza et al. 2013; 2018).

However, the two candidate compensation regions showed different patterns as a function of age and performance: whereas the frontal region showed additive effects of both variables (Figure 2C, upper), the cuneus region showed signs of an interaction ($p = 0.028$; though this would not survive correction for multiple comparisons across the two ROIs), whereby the relationship with performance was strongest in the oldest participants (and there was little sign of a performance relationship in the youngest participants; Figure 2C, lower). This is suggestive of compensatory activation only engaged by higher-performing older people in the cuneus specifically.

It has previously been shown that many effects of age on the BOLD signal measured by fMRI relate to vascular effects of ageing, rather than necessarily indicating differences in neural activity (Tsvetanov et al., 2020). We therefore repeated the multiple regressions after scaling the Cattell activation effect by an estimate of the Resting State Fluctuation Amplitude (RSFA) for each ROI from an independent, resting-state scan for each participant. Previous work has shown that RSFA relates to age-related vascular differences (Tsvetanov et al., 2015, 2020), but

not neural differences (Tsvetanov et al 2015, Kumar et al 2020). Despite this RSFA adjustment, the pattern of effects remained similar in each ROI (Table 1; Figure 2C). This suggests that these effects of age (and the relationship with performance) are neural in origin. This check has not been performed in previous fMRI studies of age-related compensation, which could reflect vascular effects of ageing instead.

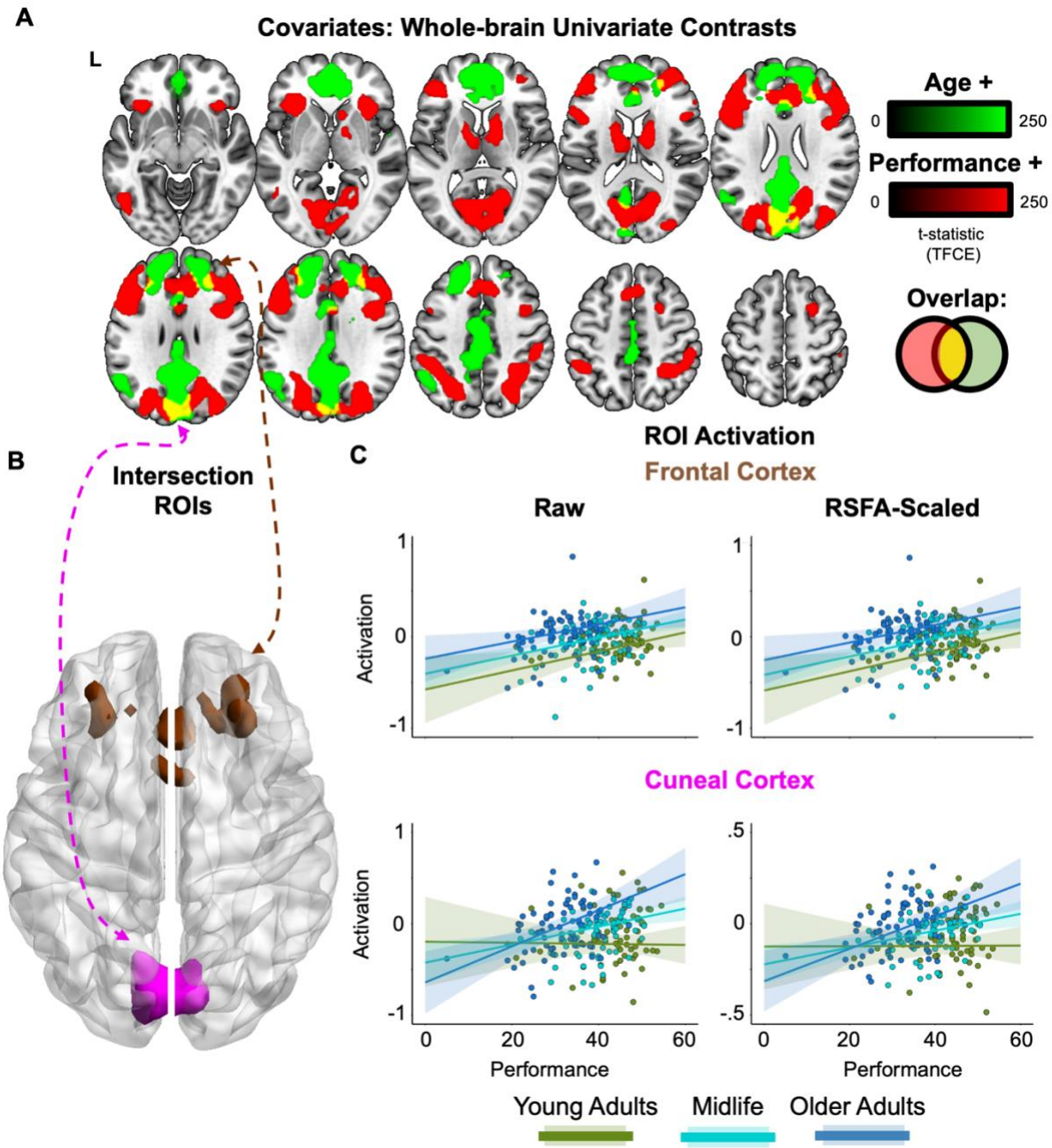

Figure 2. Univariate analysis. **(A) Whole-brain effects of age and performance.** Age (green) and performance (red) positively predicted unique aspects of increased task activation, with their spatial overlap (yellow) being overlaid on a template MNI brain, using $p < 0.05$ TFCE. **(B) Intersection ROIs.** A bilateral cuneal (magenta) and frontal cortex (brown) ROI were defined from voxels that showed a positive and unique effect of both age and performance (yellow map in Figure 2A). **(C) ROI**

Activation. Activation (raw = left; RSFA-scaled = right) is plotted against behavioural performance based on a tertile split between three age groups.

Table 1. **Standardised coefficients in multiple regression predicting fMRI activation (Hard - Easy) as a function of Age and Performance for the two ROIs identified in Figure 2**. Note that the p-values for the main effects of Age and Performance are biased by the selection of these voxels. RSFA = scaled by Resting-State Fluctuation Amplitudes (see text).

Region	Coefficient	Estimate	t value	Pr(>|t|)
Cuneal				
	Constant term	-0.06	-2.57	0.011
	Age	0.09	3.57	<.001
	Performance	0.08	3.21	0.002
	Sex	-0.05	-2.59	0.01
	Age x Performance	0.04	2.21	0.028
Cuneal (RSFA)				
	Constant term	-0.03	-2.60	0.010
	Age	0.04	3.24	0.001
	Performance	0.04	3.11	0.002
	Sex	-0.02	-2.52	0.013
	Age x Performance	0.02	1.97	0.049
Frontal				
	Constant term	-0.03	-2.02	0.045
	Age	0.08	4.24	<.001
	Performance	0.08	4.54	<.001
	Sex	<0.001	-0.35	0.728
	Age x Performance	<0.001	-0.15	0.882
Frontal (RSFA)				
	Constant term	-0.02	-1.99	0.048
	Age	0.04	4.12	<.001
	Performance	0.04	4.48	<.001
	Sex	0.00	-0.37	0.709

Age x Performance	0.00	-0.13	0.898

Multivariate Bayesian Decoding

Next, we examined if these candidate compensation regions showed multivariate evidence of compensation. If their age- and performance-related activation reflects compensation, then multivoxel analyses should show that this “hyperactivation” carries additional information about the task, over and above that already provided by the regions generally activated by the task (i.e., MDN). To test this, we applied Multivariate Bayesian decoding (MVB) of the [Hard > Easy] contrast.

We first implemented MVB with a ‘joint model’ that contained voxel activation patterns from (1) one of the potential compensation ROIs and (2) the same number of the most significant voxels in the MDN (defined by the orthogonal contrast of [Hard > Easy]; Figure 1C; see Table 2 for voxel numbers). For each joint model (i.e., MDN voxels + cuneal or frontal voxels), we compared the log model evidence for the correct model to ones where the stimulus onsets were shuffled (i.e., to estimate a null distribution of model evidence). Across both joint models (MDN plus cuneal or frontal cortex), we found evidence of above-chance decoding (real vs. shuffled log-evidence difference > 3; see Methods) for all except two participants. These participants (the two points below the y = 3 dashed line in Figure 3A, one of whom was the same across models) were removed (Morcom & Henson, 2018; Knights et al., 2021).

Having established that the task condition could be decoded from voxels in the vast majority of participants, the critical test was whether age influenced the likelihood that adding voxel activation patterns from the ‘compensatory’ ROIs (i.e., joint model) would boost decoding accuracy relative to that for the MDN-only model. A positive age effect on boost likelihood would indicate that, the older someone was, the more likely that activation patterns in the putative “compensation ROI” would

provide additional, non-redundant, task-relevant information, consistent with a compensatory role. In line with this compensation account, there was a significant positive effect of age (Table 2) on the likelihood that model performance was boosted (i.e., log evidence change > 3) by including voxel activation patterns from the cuneal ROI (Figure 3B lower; Odds ratio = 2.21). In other words, the amount of unique task information in the multi-voxel pattern within the cuneal ROI (above that present in the MDN) increased with age. By contrast, this analysis for the model containing the frontal ROI voxel activation patterns showed no effect of age (Table 2; Figure 3B upper).

Note that, since this age effect in the cuneus was present even though the logistic regression model contained this ROI's univariate response as a covariate of no interest (Table 2), the effect of age on boost likelihood is unlikely to be due to differences in the overall signal-to-noise ratio across ages.

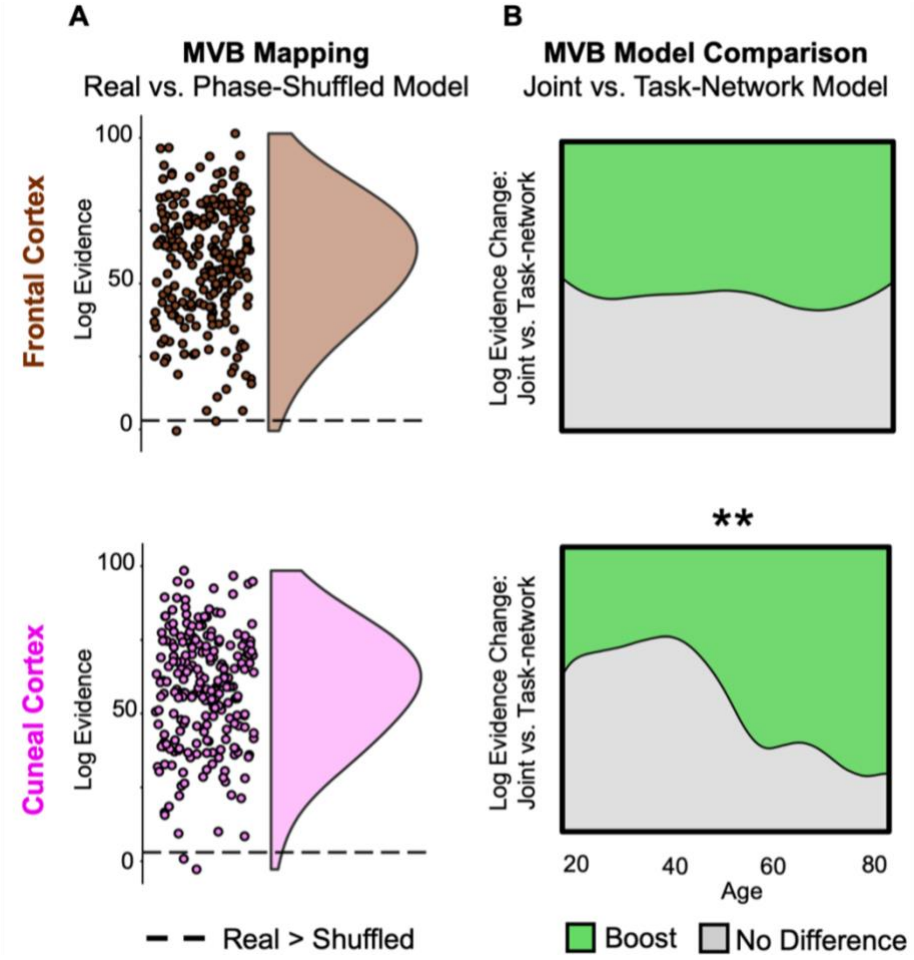

Figure 3. Multivariate Analysis. **(A) MVB Decoding.** Points represent the difference in log evidence per participant (for the real vs. shuffled model) for the joint model using activation patterns to decode the [Hard > Easy] contrast. **(B) Boost Likelihood Model Comparison.** Across age, a smoothed density estimate represents the likelihood that there was a boost (of log-evidence > 3; green) or no difference (grey) to model evidence per participant when decoding models included activation patterns from either of the compensation ROIs (Figure 2B) in addition to the MDN (Figure 1C), relative to a model that sampled only from the MDN. A significant positive linear effect of age on boost likelihood was observed for the cuneal (lower) but not frontal ROI (upper).

Table 2. Standardised coefficients in multiple logistic regression predicting **MVB Boost likelihood as a function of age** (with Sex and Mean Univariate Activation as covariates)**.**

Model	Coefficient	Estimate	z-statistic	p
Cuneal ROI + Task-network (166 voxels each)				
	Constant term	2.17	8.79	<.001
	Age	0.79	3.23	<.001
	Sex	0.08	0.37	0.714
	Univariate	-0.34	-1.59	0.112
Frontal ROI + Task-network (85 voxels each)				
	Constant term	2.20	9.30	<.001
	Age	0.04	0.19	0.851
	Sex	0.26	1.13	0.257
	Univariate	-0.54	-2.33	0.020

Discussion

The existence of age-related functional compensation mechanisms remains a matter of debate in the cognitive neuroscience of healthy ageing. Here, we analysed fMRI data from a problem-solving (fluid intelligence) task and identified two brain regions (in bilateral cuneal and frontal cortex; Figure 2A/B) that satisfied traditional univariate criteria for functional compensation. After applying the multivariate criterion that a compensating region should possess additional information about the task, only the cuneal cortex showed an age-related increase in this additional information (Figure 3B), beyond that available in the generic task-activated regions (i.e., the MDN; Figure 1C). This is the first demonstration of increased multivariate information with age, since previous studies have shown evidence for no such multivariate increase associated with univariate age-related hyper-activation in other ROIs and tasks; leading to previous findings being interpreted in terms of neural inefficiency, rather than compensation (Morcom & Henson, 2018; Knights et al., 2021).

Why would the cuneal cortex demonstrate functional compensation when solving difficult visuospatial problems? Since the cuneus has a well-established role in visual attention (e.g., Corbetta et al., 1998), we hypothesise that the additional recruitment of this brain region facilitates concurrently attending to multiple features of the stimulus array, to correctly select the ‘odd-one-out’. The recruitment of this brain region in older adults could drive changes in looking strategy (e.g., Law et al., 1996), where, for example, older adults compensate for their reduced visual short-term memory (Mitchell et al., 2018) - i.e., difficulty sustaining representations of puzzle items - by using more or different saccades. This possibility is consistent with the greater cuneal activation that was observed for older adults who performed better at the task (Figure 2C). Future work pairing fMRI behavioural tasks with eye-

monitoring could verify this proposed relationship between age, cuneus activation, overt attention and fluid intelligence.

In line with this hypothesised role of the cuneal cortex, there is consistent functional (Yin et al., 2015; Santarnecchi et al., 2017) and structural (Haier et al., 2004; Jauk et al., 2015; Chen et al. 2020) neuroimaging evidence that link this brain region to aspects of fluid intelligence like rule-application. Similarly, responses from sensory areas (like the secondary visual network that overlaps our cuneus ROI; Ji et al., 2019) have been shown to predict fluid intelligence performance (Brumback et al., 2004). In aging, it is well established that sensory and intellectual decline are correlated (see Baltes & Lindenberger, 1997), either because they share a common cause or because performance of fluid intelligence tasks is partially dependent on sensory processing (e.g., Schneider & Pichora-Fuller, 2000). While our data cannot tease apart these hypotheses, it may be that compensatory processes in the cuneal region reflect this shared age-related variance between sensory and higher-order cognitive tasks.

Though activation of the cuneal ROI increased with age, it is worth noting the constant term (reflecting the average across all ages) was negative (Table 1), suggesting that most people (other than the older ones) showed greater activation of this region for easy than hard problems. This is more difficult to reconcile with its activation reflecting visual attention or eye movements, since this would suggest greater visual attention/eye movements toward easy than hard problems in the young. One alternative possibility is active suppression of the cuneal region in the hard blocks, to avoid distraction (e.g., minimise attentional capture from neighbouring display panels while processing features in each panel). Thus, the age-related reduction in the Easy-Hard difference (leading to the positive correlation of

the Hard-Easy difference with age) could reflect reduced ability to inhibit the cuneus during hard problems, consistent with the established age-related decline in the ability to suppress distracting information in complex stimuli (Tsvetanov et al., 2013, Rey-Mermet et al., 2018, Bouhassoun et al., 2022). However, it is not clear why this alternative account would predict a positive correlation between cuneal activity and task performance, given that greater suppression (in the Hard condition) would be expected to lead to better performance, but more negative activity values for the [Hard - Easy] contrast. Thus, we favour the explanation in terms of functional compensation.

Another possibility is that the age-related increases in fMRI activations (for hard versus easy) in one or both of our ROIs do not reflect greater fMRI signal for hard problems in older than younger people, but rather lower fMRI signal for easy problems in the older. Without a third baseline condition, we cannot distinguish these two possibilities in our data. However, a reduced “baseline” level of fMRI signal (e.g., for easy problems) in older people is consistent with other studies showing an age-related decline in baseline perfusion levels, coupled with preserved capacity of cerebrovascular reactivity to meet metabolic demands of neuronal activity at higher cognitive load (Calautti et al., 2001; Jennings et al., 2005). Though age-related decline in baseline perfusion occurs in the cuneal cortex (Tsvetanov et al., 2021), the brain regions showing modulation of behaviourally-relevant Cattell fMRI activity by perfusion levels did not include the cuneal cortex (Wu et al., 2021). This suggests that the compensatory effects in the cuneus are unlikely to be explained by age-related hypo-perfusion, consistent with the minimal effect here of adjusting for RSFA (Figure 2C).

The age- and performance-related activation in our frontal region satisfied the traditional univariate criteria for functional compensation, but our multivariate (MVB) analysis showed that additional multivariate information was absent in this region, which is inconsistent with compensation. This pattern of results suggests that traditional univariate criteria alone are not sufficient for identifying functional compensation. Similar univariate effects have been found in previous studies (though with smaller samples), where lateral and medial frontal areas show increased activation during healthy ageing across a range of tasks, including those related to executive control or attention (e.g., Grady et al., 2010; for a review, see Spreng et al., 2010; also see Raz et al., 2008, for a neuroanatomical link). Patients with brain damage also demonstrate increased frontal activation during language and semantic processing (Brownsett et al., 2014; Rice et al., 2018) indicating that this mechanism might be a response to brain atrophy generally. Instead, our results suggest that this frontal hyperactivation in older adults reflects “inefficient” processing, in terms of more neural resources being needed to perform the task (i.e., for hard versus easy problems). In fact, neural inefficiency was our favoured interpretation of previous cases when MVB showed no age-related boost, in frontal (Morcom & Henson, 2018) or motor (Knights et al., 2021) regions. From these studies, and all previous fMRI/PET studies that showed age-related hyper-activation, it was not known whether the increased activations reflected greater neural inefficiency, or greater haemodynamic resources needed for the same level of neural activity (i.e., vascular rather than neural inefficiency). Here, we showed for the first time that the age-related increase in both ROIs remained even after adjusting for RSFA (Table 1), suggesting that this hyper-activation reflects neural rather than vascular inefficiency.

In Morcom & Henson (2018), we did not explicitly test for a relationship between activation and (memory) performance, and in Knights et al. (2021), we failed to find any relationship between (ipsilateral motor) activation and various (motor) performance measures. In the present study, it may be that the age-related frontal hyper-activation is caused by neural inefficiency, yet the degree of overall activation still relates to (lifespan-stable) problem-solving performance. Converging with the lack of additional multivariate information, this suggests that the frontal region does not show a compensatory response.

In summary, we propose that our results in the cuneus represent the most compelling evidence to date for functional compensation in healthy ageing, with further work needed to determine the precise function of this region in problem-solving tasks like that examined here. Together with the results in prefrontal cortex, the data also suggest that specific compensatory neural responses can coexist with inefficient neural function in older people.

Methods

Participants

A healthy population-derived adult lifespan human sample (N = 223; ages approximately uniformly distributed from 19 - 87 years; females = 112; 50.2%) was collected as part of the Cam-CAN study (Stage 3 cohort; Shafto et al., 2014). Participants were fluent English speakers in good physical and mental health, based on the Cam-CAN cohort's exclusion criteria which includes poor mini mental state examination, ineligibility for MRI and medical, psychiatric, hearing or visual problems. Throughout analyses, age is defined at the Home Interview (Stage 1; Shafto et al., 2014). The study was approved by the Cambridgeshire 2 (now East of England–Cambridge Central) Research Ethics Committee and participants provided informed written consent.

Materials & Procedure

A modified version of the odd-one-out subtest of the standardised Cattell Culture Fair Intelligence test (Scale 2; Cattell, 1971; Cattell & Cattell, 1973) was developed for use in the scanner (Woolgar et al., 2013; Samu et al., 2017; Wu et al., 2021). Participants were scanned while performing the problem-solving task where, on each trial, four display panels were presented in a horizontal row (Figure 1A) in the centre of a screen that was viewed through a head-coil mounted mirror. Participants were required to make a button press response to identify the mismatching panel that was unique in some way from the other three (based on either a figural, spatial, complex, or abstract property).

In a block design, participants completed eight 30-second blocks which contained a series of puzzles from one of two difficulty levels (i.e., four hard and four

easy blocks completed in an alternating block order; Figure 1A). The fixed block time allowed participants to attempt as many trials as possible. Therefore, to balance speed and accuracy, behavioural performance was measured by subtracting the number of incorrect from correct trials and averaging over the hard and easy blocks independently (i.e., ((hard correct - hard incorrect) + (easy correct - easy incorrect))/2; Samu et al., 2017). For assessing reliability and validity, behavioural performance (total number of puzzles correct) was also collected from the same participants during a full version of the Cattell task (Scale 2 Form A) administered outside the scanner at Stage 2 of the Cam-CAN study (Shafto et al., 2014). Both the in- and out-of-scanner measures were z-scored. As with Samu et al (2017), we did not include participants (N = 28; 17 females) who performed poorly on the fMRI task, defined as 10 or more hard incorrect trials, roughly equivalent to >50% errors).

Data Acquisition & Preprocessing

The MRI data were collected using a Siemens 3T TIM TRIO system with a 32 channel head-coil. A T2*-weighted echoplanar imaging (EPI) sequence was used to collect 150 volumes, each containing 32 axial slices (acquired in descending order) with slice thickness of 3.0mm and an interslice gap of 25% for whole brain coverage (TR = 2000ms; TE = 30ms; flip angle = 78°; FOV = 192mm x 192mm; voxel-size 3 x 3 x 3.75mm). Higher resolution (1mm x 1mm x 1mm) T1- and T2-weighted structural images were also acquired (to aid registration across participants).

MR data preprocessing and univariate analysis were performed with SPM12 software (Wellcome Department of Imaging Neuroscience, London, www.fil.ion.ucl.ac.uk/spm), release 4537, implemented in the AA 4.0 pipeline (Cusack et al., 2015) described in Taylor et al. (2017). Specifically, structural images were rigid-body registered to an MNI template brain, bias corrected, segmented, and warped to match a grey matter template created from the whole Cam-CAN Stage 2 sample using DARTEL (Ashburner, 2007; Taylor et al., 2017). This template was subsequently affine transformed to standard Montreal Neurological Institute (MNI) space. The functional images were spatially realigned, interpolated in time to correct for the different slice acquisition times, rigid-body coregistered to the structural image, transformed to MNI space using the warps and affine transforms from the structural image, and resliced to 3mm x 3mm x 3mm voxels.

Univariate Analysis

For participant-level modelling, a regressor for each condition was created by convolving boxcar functions of 30 sec duration for each block with SPM's canonical haemodynamic response function. Additional regressors were included in each GLM to capture residual movement-related artifacts, including six representing the x/y/z

rigid body translations and rotations (estimated in the realignment stage). Finally, the data were scaled to a grand mean of 100 over all voxels and scans within a session, and the model was fit to the data in each voxel. The autocorrelation of the error was estimated using an AR(1)-plus-white-noise model, together with a set of cosines that functioned to high-pass filter the model and data to 1/128 Hz, that were estimated using restricted maximum likelihood. The estimated error autocorrelation was then used to “prewhiten” the model and data, and ordinary least squares used to estimate the model parameters. The contrast of parameter estimates for the hard and easy conditions, per voxel and participant, was then calculated and combined in a group GLM with independent regressors for age and in-scanner behavioural performance.

ROIs

All ROIs were defined by selecting activated voxels from a group-level GLM (see Table 2 for number of voxels within ROIs). The two ROIs that were tested as candidate regions for functional compensation (i.e., cuneal cortex and frontal cortex) were defined by contiguous voxels that were significantly positively related to the independent effects of both age and performance (see Figure 2). The MDN was defined by the selecting suprathreshold voxels activated by the [Hard vs. Easy] contrast from the Cattell task. For MVB analysis (see below), a subset of the highest activated voxels within the MDN were taken to match the number of voxels with that of the “compensation ROI” being tested (see Figure 3; Table 2).

For the ROI-based multiple regressions, the activation was averaged across voxels (i.e., mean difference in parameter estimates for Hard – Easy conditions) for each ROI and participant (Figure 2, Table 2). In the case of RSFA-scaled multiple regression, we used RSFA calculated from independent resting state scans (see Tsvetanov et al., 2015) to scale the task-related BOLD response (by dividing the

Hard – Easy difference in parameter estimates for each voxel by the RSFA value at the same voxel).

MVB

A series of MVB models were fit to assess the information about task condition that was represented in each ROI or combination of ROIs. Each MVB decoding model is based on the same design matrix of experimental variables used in the univariate GLM, but the mapping is reversed; many physiological data features (fMRI activity in multiple voxels) are used to predict a psychological target variable (Friston et al., 2008). This target (outcome) variable is specified as the contrast [Hard > Easy] with all covariates removed from the predictor variables.

Each MVB model was fit using a parametric empirical Bayes approach, in which empirical priors on the data features (voxelwise activity) are specified in terms of spatial patterns over voxel features and the variances of the pattern weights. As in earlier work (Morcom & Henson, 2018; Knights et al., 2021), we used a sparse spatial prior in which “patterns” are individual voxels. Since these decoding models are normally ill-posed (with more voxels than scans), these spatial priors on the patterns of voxel weights regularize the solution.

The pattern weights specifying the mapping of data features to the target variable are optimized with a greedy search algorithm using a standard variational scheme (Friston et al., 2007). This is achieved by maximizing the free energy, which provides an upper bound on the log of the Bayesian model evidence (the marginal probability of the data given that model). The evidence for different models predicting the same psychological variable can then be compared by computing the difference in log evidences, which is equivalent to the log of the Bayes factor (Friston et al., 2008; Chadwick et al., 2012; Morcom & Friston, 2012).

The outcome measure was the log evidence for each model (Morcom & Henson, 2018; Knights et al., 2021). To test whether activity from an ROI is compensatory, we used an ordinal boost measure (Morcom & Henson, 2018; Knights et al., 2021) to assess the contribution of that ROI for the decoding of task-relevant information (Figure 3B). Specifically, Bayesian model comparison assessed whether a model that contains activity patterns from a compensatory ROI and the MDN (i.e., a joint model) boosted the prediction of task-relevant information relative to a model containing the MDN only. The compensatory hypothesis predicts that the likelihood of a boost to model decoding will increase with older age. The dependent measure, for each participant, was a categorical recoding of the relative model evidence to indicate the outcome of the model comparison. The three possible outcomes were: a boost to model evidence for the joint vs. MDN-only model (difference in log evidence > 3), ambiguous evidence for the two models (difference in log evidence between -3 to 3), or a reduction in evidence for the joint vs. MDN-only model (difference in log evidence < -3). These values were selected because a log difference of three corresponds to a Bayes Factor of 20, which is generally considered strong evidence (Lee & Wagenmakers, 2014). A reduction in model evidence was not observed in the current study.

For this MVB boost analysis, participants were only included if their data allowed reliable decoding by the joint model (Morcom & Henson, 2018; Knights et al., 2021). To determine this, we contrasted the log evidence for the joint model with that from models in which the design matrix (and therefore the target variable) was randomly phase shuffled 20 times. The definition of reliable was based on a mean of 3 or more in the difference of log-evidence between the true and shuffled model (Morcom & Henson, 2018; Fig. 3A). Note that decoding is performed after removing

the mean across voxels (i.e., MVB results are independent of the results in the univariate analyses presented in Fig 1C & Table 1).

Experimental Design & Statistical Analysis

Continuous age and behavioural performance variables were standardised and treated as linear predictors in multiple regression throughout the behavioural, univariate (Table 1, Figure 1B/2A) and MVB boost (Table 2) analyses. Sex was included as a covariate. For whole-brain voxelwise analyses, clusters were estimated using threshold-free cluster enhancement (TFCE; Smith & Nichols 2009) with 2000 permutations. Bonferroni correction was applied to a standard alpha = 0.05 based on the two ROIs (cuneal and frontal) that were examined. For Bayes Factors, interpretation criteria norms were drawn from Jarosz & Wiley (2014).

Data Availability

Raw and minimally pre-processed MRI (i.e., from automatic analysis; Taylor et al., 2017) and behavioural data are available by submitting a data request to Cam-CAN (https://camcan-archive.mrc-cbu.cam.ac.uk/dataaccess/). The univariate and multivariate ROI data, and behavioural data, can be downloaded from the Open Science Framework (https://osf.io/v7kmh) while the analysis code is available on GitHub (https://github.com/ethanknights/Knightsetal_fMRI-Cattell-Compensation).

References

Ashburner, J. (2007). A fast diffeomorphic image registration algorithm. Neuroimage, 38(1), 95-113.

Baltes, P. B., & Lindenberger, U. (1997). Emergence of a powerful connection between sensory and cognitive functions across the adult life span: a new window to the study of cognitive aging?. Psychology and aging, 12(1), 12.

Bors, D. A., & Forrin, B. (1995). Age, speed of information processing, recall, and fluid intelligence. Intelligence, 20(3), 229-248.

Bouhassoun, S., Poirel, N., Hamlin, N., & Doucet, G. E. (2022). The forest, the trees, and the leaves across adulthood: Age-related changes on a visual search task containing three-level hierarchical stimuli. Attention, Perception, & Psychophysics, 1-12.

Brownsett, S. L., Warren, J. E., Geranmayeh, F., Woodhead, Z., Leech, R., & Wise, R. J. (2014). Cognitive control and its impact on recovery from aphasic stroke. Brain, 137(1), 242-254.

Brumback, C. R., Low, K. A., Gratton, G., & Fabiani, M. (2004). Sensory ERPs predict differences in working memory span and fluid intelligence. Neuroreport, 15(2), 373-376.

Cabeza, R. (2002). Hemispheric asymmetry reduction in older adults: the HAROLD model. Psychology and aging, 17(1), 85.

Cabeza, R. & Dennis, N. A. in Principles of Frontal Lobe Function (eds Stuss, D. T. & Knight, R. T.) (Oxford Univ. Press, New York, 2013).

Cabeza, R., Albert, M., Belleville, S., Craik, F. I., Duarte, A., Grady, C. L., ... & Rajah, M. N. (2018). Maintenance, reserve and compensation: the cognitive neuroscience of healthy ageing. Nature Reviews Neuroscience, 19(11), 701-710.

Calautti, C., Serrati, C., & Baron, J. C. (2001). Effects of age on brain activation during auditory-cued thumb-to-index opposition: a positron emission tomography study. Stroke, 32(1), 139-146.

Cattell, R.B. (1971). Abilities: Their Structure, Growth, and Action. Houghton Mifflin, Boston.

Cattell, R.B., & Cattell, H. E. P. (1973). Measuring Intelligence with the Culture Fair Tests. The Institute for Personality and Ability Testing, Champaign, IL

Chadwick MJ, Bonnici HM, Maguire EA (2012) Decoding information in the human hippocampus: a user's guide. Neuropsychologia 50:3107–3121.

Chen, P. Y., Chen, C. L., Hsu, Y. C., & Tseng, W. Y. I. (2020). Fluid intelligence is associated with cortical volume and white matter tract integrity within multiple-demand system across adult lifespan. NeuroImage, 212, 116576.

Christensen, K., Doblhammer, G., Rau, R., & Vaupel, J. W. (2009). Ageing populations: the challenges ahead. The Lancet, 374(9696), 1196-1208.

Clay, O. J., Edwards, J. D., Ross, L. A., Okonkwo, O., Wadley, V. G., Roth, D. L., & Ball, K. K. (2009). Visual function and cognitive speed of processing mediate age-related decline in memory span and fluid intelligence.

Colom, R., Haier, R. J., Head, K., Álvarez-Linera, J., Quiroga, M. Á., Shih, P. C., & Jung, R. E. (2009). Gray matter correlates of fluid, crystallized, and spatial intelligence: Testing the P-FIT model. Intelligence, 37(2), 124-135.

Corbetta, M., Akbudak, E., Conturo, T. E., Snyder, A. Z., Ollinger, J. M., Drury, H. A., ... & Shulman, G. L. (1998). A common network of functional areas for attention and eye movements. Neuron, 21(4), 761-773.

Crittenden, B. M., Mitchell, D. J., & Duncan, J. (2016). Task encoding across the multiple demand cortex is consistent with a frontoparietal and cingulo-opercular dual networks distinction. Journal of Neuroscience, 36(23), 6147-6155.

Cusack, R., Vicente-Grabovetsky, A., Mitchell, D. J., Wild, C. J., Auer, T., Linke, A. C., & Peelle, J. E. (2015). Automatic analysis (aa): efficient neuroimaging workflows and parallel processing using Matlab and XML. Frontiers in neuroinformatics, 8, 90.

Deary, I. J. (2012). Intelligence. Annual Review Psycholology 63,453–482.

Duncan, J., & Owen, A. M. (2000). Common regions of the human frontal lobe recruited by diverse cognitive demands. Trends in neurosciences, 23(10), 475-483.

Duncan, J. (2010). The multiple-demand (MD) system of the primate brain: mental programs for intelligent behaviour. Trends in cognitive sciences, 14(4), 172-179.

Friston, K., Chu, C., Mourão-Miranda, J., Hulme, O., Rees, G., Penny, W., & Ashburner, J. (2008). Bayesian decoding of brain images. Neuroimage, 39(1), 181-205.

Ghisletta, P., Rabbitt, P., Lunn, M., & Lindenberger, U. (2012). Two thirds of the age-based changes in fluid and crystallized intelligence, perceptual speed, and memory in adulthood are shared. Intelligence, 40(3), 260-268.

Gray, J. R., Chabris, C. F., & Braver, T. S. (2003). Neural mechanisms of general fluid intelligence. Nature neuroscience, 6(3), 316-322.

Haier, R. J., Jung, R. E., Yeo, R. A., Head, K., & Alkire, M. T. (2004). Structural brain variation and general intelligence. Neuroimage, 23(1), 425-433.

Jarosz, A. F., & Wiley, J. (2014). What are the odds? A practical guide to computing and reporting Bayes factors. The Journal of Problem Solving, 7(1), 2.

Jauk, E., Neubauer, A. C., Dunst, B., Fink, A., & Benedek, M. (2015). Gray matter correlates of creative potential: A latent variable voxel-based morphometry study. NeuroImage, 111, 312-320.

Jennings, J. R., Muldoon, M. F., Ryan, C., Price, J. C., Greer, P., Sutton-Tyrrell, K., ... & Meltzer, C. C. (2005). Reduced cerebral blood flow response and compensation among patients with untreated hypertension. Neurology, 64(8), 1358-1365.

Ji, J. L., Spronk, M., Kulkarni, K., Repovš, G., Anticevic, A., & Cole, M. W. (2019). Mapping the human brain's cortical-subcortical functional network organization. Neuroimage, 185, 35-57.

Kievit, R. A., Davis, S. W., Mitchell, D. J., Taylor, J. R., Duncan, J., & Henson, R. N. (2014). Distinct aspects of frontal lobe structure mediate age-related differences in fluid intelligence and multitasking. Nature communications, 5(1), 1-10.

Kievit, R. A., Fuhrmann, D., Borgeest, G. S., Simpson-Kent, I. L., & Henson, R. (2018). The neural determinants of age-related changes in fluid intelligence: a pre-registered, longitudinal analysis in UK Biobank. Wellcome open research, 3, 38. https://doi.org/10.12688/wellcomeopenres.14241.2

Knights, E., Morcom, A. M., & Henson, R. N. (2021). Does Hemispheric Asymmetry Reduction in Older Adults in Motor Cortex Reflect Compensation?. Journal of Neuroscience, 41(45), 9361-9373.

Kumral, D., Şansal, F., Cesnaite, E., Mahjoory, K., Al, E., Gaebler, M., ... & Villringer, A. (2020). BOLD and EEG signal variability at rest differently relate to aging in the human brain. Neuroimage, 207, 116373.

Law, I., Svarer, C., & Paulson, O. B. (1996). The activation pattern during eye movements. Electroencephalography and Clinical Neurophysiology, 4(99), 394.

Lee, K. H., Choi, Y. Y., Gray, J. R., Cho, S. H., Chae, J. H., Lee, S., & Kim, K. (2006). Neural correlates of superior intelligence: stronger recruitment of posterior parietal cortex. Neuroimage, 29(2), 578-586.

Lee, M. D., & Wagenmakers, E. J. (2014). Bayesian cognitive modeling: A practical course. Cambridge UP.

Lövdén, M., Bäckman, L., Lindenberger, U., Schaefer, S., & Schmiedek, F. (2010). A theoretical framework for the study of adult cognitive plasticity. Psychological bulletin, 136(4), 659.

Mitchell, D. J., Cusack, R., & Cam-CAN. (2018). Visual short-term memory through the lifespan: Preserved benefits of context and metacognition. Psychology and Aging, 33(5), 841-854.

Mitchell, D. J., Mousley, A. L., Shafto, M. A., & Duncan, J. (2023). Neural contributions to reduced fluid intelligence across the adult lifespan. Journal of Neuroscience, 43(2), 293-307.

Morcom, A. M., & Friston, K. J. (2012). Decoding episodic memory in ageing: a Bayesian analysis of activity patterns predicting memory. Neuroimage, 59(2), 1772-1782.

Morcom, A. M., & Henson, R. N. (2018). Increased prefrontal activity with aging reflects nonspecific neural responses rather than compensation. Journal of Neuroscience, 38(33), 7303-7313.

Paul, E. J., Larsen, R. J., Nikolaidis, A., Ward, N., Hillman, C. H., Cohen, N. J., ... & Barbey, A. K. (2016). Dissociable brain biomarkers of fluid intelligence. Neuroimage, 137, 201-211.

Raz, N., Lindenberger, U., Ghisletta, P., Rodrigue, K. M., Kennedy, K. M., & Acker, J. D. (2008). Neuroanatomical correlates of fluid intelligence in healthy adults and persons with vascular risk factors. Cerebral cortex, 18(3), 718-726.

Rey-Mermet, A., & Gade, M. (2018). Inhibition in aging: What is preserved? What declines? A meta-analysis. Psychonomic bulletin & review, 25, 1695-1716.

Rice, G. E., Caswell, H., Moore, P., Lambon Ralph, M. A., & Hoffman, P. (2018). Revealing the dynamic modulations that underpin a resilient neural network for semantic cognition: an fMRI investigation in patients with anterior temporal lobe resection. Cerebral Cortex, 28(8), 3004-3016.

Salthouse, T. A., & Pink, J. E. (2008). Why is working memory related to fluid intelligence?. Psychonomic bulletin & review, 15(2), 364-371.

Salthouse, T. A., Pink, J. E., & Tucker-Drob, E. M. (2008). Contextual analysis of fluid intelligence. Intelligence, 36(5), 464-486.

Samu, D., Campbell, K. L., Tsvetanov, K. A., Shafto, M. A., & Tyler, L. K. (2017). Preserved cognitive functions with age are determined by domain-dependent shifts in network responsivity. Nature communications, 8(1), 1-14.

Santarnecchi, E., Emmendorfer, A., & Pascual-Leone, A. (2017). Dissecting the parieto-frontal correlates of fluid intelligence: A comprehensive ALE meta-analysis study. Intelligence, 63, 9-28.

Schneider, B. A. & Pichora-Fuller, M. K. (2000). Implications of perceptual deterioration for cognitive aging research. In: Handbook of cognitive aging II (Craik, F. I. M & Salthouse, T. A., Eds.), Mahwah, NJ: Erlabum.

Schretlen, D., Pearlson, G. D., Anthony, J. C., Aylward, E. H., Augustine, A. M., Davis, A., & Barta, P. (2000). Elucidating the contributions of processing speed, executive ability, and frontal lobe volume to normal age-related differences in fluid intelligence. Journal of the International Neuropsychological Society, 6(1), 52-61.

Shafto, M. A., Tyler, L. K., Dixon, M., Taylor, J. R., Rowe, J. B., Cusack, R., ... & Matthews, F. E. (2014). The Cambridge Centre for Ageing and Neuroscience (Cam-CAN) study protocol: a cross-sectional, lifespan, multidisciplinary examination of healthy cognitive ageing. BMC neurology, 14(1), 1-25.

Smith, V., Duncan, J., & Mitchell, D. J. (2021). Roles of the default mode and multiple-demand networks in naturalistic versus symbolic decisions. Journal of Neuroscience, 41(10), 2214-2228.

Smith, S. M., & Nichols, T. E. (2009). Threshold-free cluster enhancement: addressing problems of smoothing, threshold dependence and localisation in cluster inference. Neuroimage, 44(1), 83-98.

Spreng, R. N., Wojtowicz, M., & Grady, C. L. (2010). Reliable differences in brain activity between young and old adults: a quantitative meta-analysis across multiple cognitive domains. Neuroscience & Biobehavioral Reviews, 34(8), 1178-1194.

Taylor, J. R., Williams, N., Cusack, R., Auer, T., Shafto, M. A., Dixon, M., ... & Henson, R. N. (2017). The Cambridge Centre for Ageing and Neuroscience (Cam-CAN) data repository: Structural and functional MRI, MEG, and cognitive data from a cross-sectional adult lifespan sample. neuroimage, 144, 262-269.

Tsvetanov, K. A., Henson, R. N., Jones, P. S., Mutsaerts, H., Fuhrmann, D., Tyler, L. K., ... & Rowe, J. B. (2021). The effects of age on resting-state BOLD signal variability is explained by cardiovascular and cerebrovascular factors. Psychophysiology, 58(7), e13714.

Tsvetanov, K. A., Henson, R. N., & Rowe, J. B. (2021). Separating vascular and neuronal effects of age on fMRI BOLD signals. Philosophical Transactions of the Royal Society B, 376(1815), 20190631.

Tsvetanov, K. A., Henson, R. N., Tyler, L. K., Davis, S. W., Shafto, M. A., Taylor, J. R., ... & Rowe, J. B. (2015). The effect of ageing on f MRI: Correction for the confounding effects of vascular reactivity evaluated by joint f MRI and MEG in 335 adults. Human brain mapping, 36(6), 2248-2269.

Tsvetanov, K. A., Mevorach, C., Allen, H., & Humphreys, G. W. (2013). Age-related differences in selection by visual saliency. Attention, Perception, & Psychophysics, 75(7), 1382-1394.

Tschentscher, N., Mitchell, D., & Duncan, J. (2017). Fluid intelligence predicts novel rule implementation in a distributed frontoparietal control network. Journal of Neuroscience, 37(18), 4841-4847.

Woolgar, A., Bor, D., & Duncan, J. (2013). Global increase in task-related fronto-parietal activity after focal frontal lobe lesion. Journal of cognitive neuroscience, 25(9), 1542-1552.

Wu, S., Tyler, L. K., Henson, R. N., Rowe, J. B., & Tsvetanov, K. A. (2023). Cerebral blood flow predicts multiple demand network activity and fluid intelligence across the adult lifespan. Neurobiology of aging, 121, 1-14.

Yin, S., Zhu, X., He, R., Li, R., & Li, J. (2015). Spontaneous activity in the precuneus predicts individual differences in verbal fluency in cognitively normal elderly. Neuropsychology, 29(6), 961.

Zamroziewicz, M. K., Paul, E. J., Zwilling, C. E., & Barbey, A. K. (2018). Determinants of fluid intelligence in healthy aging: Omega-3 polyunsaturated fatty acid status and frontoparietal cortex structure. Nutritional neuroscience, 21(8), 570-579.

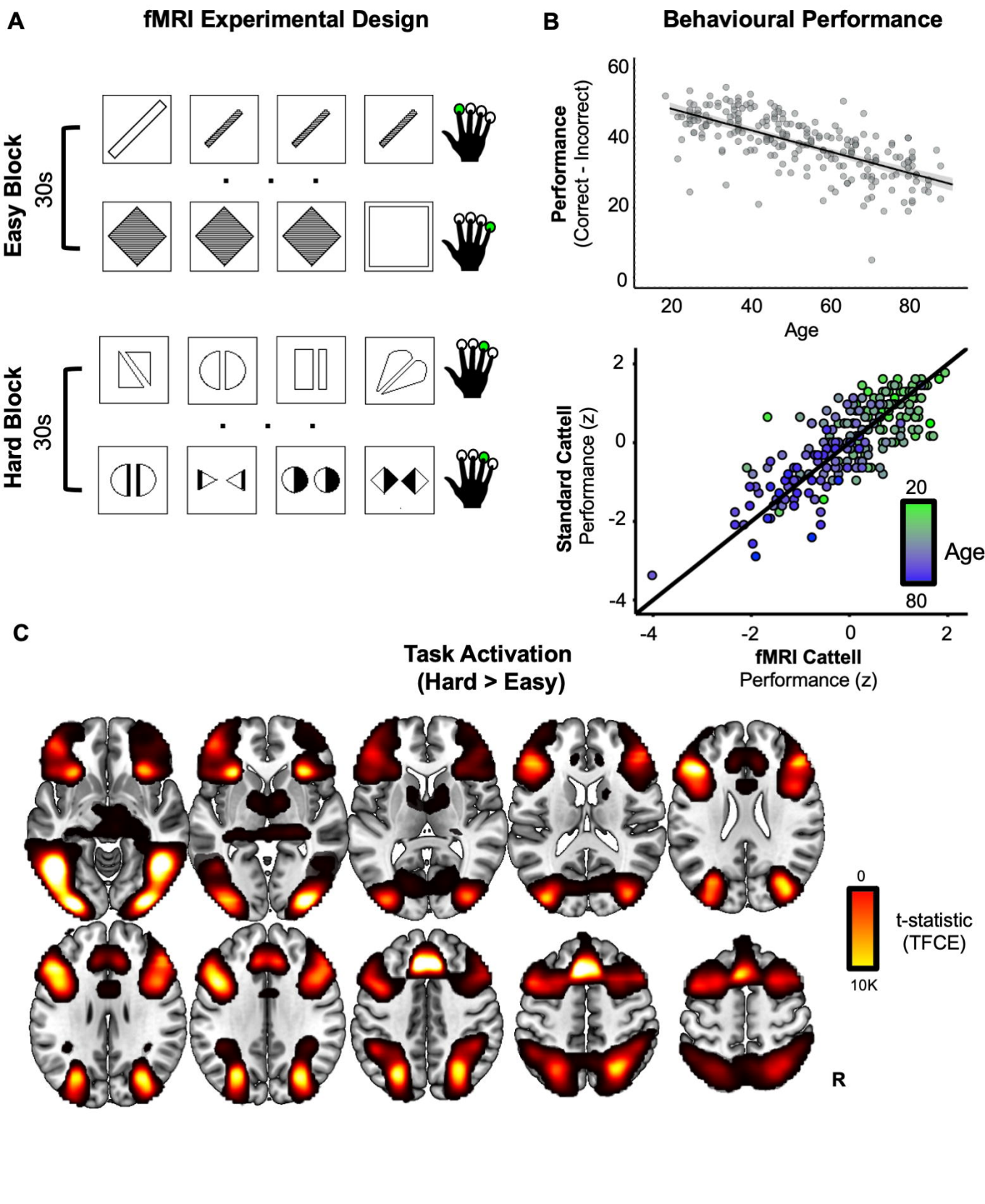
A
fMRI Experimental Design
Easy Block
30s
Hard Block
30s
B
Behavioural Performance
Performance
(Correct - Incorrect)
60
40
20
0
20
40
60
80
Age
Standard Cattell
Performance (z)
2
0
-2
-4
20
Age
80
-4
-2
0
2
fMRI Cattell
Performance (z)
C
Task Activation
(Hard > Easy)
0
t-statistic
(TFCE)
10K
R

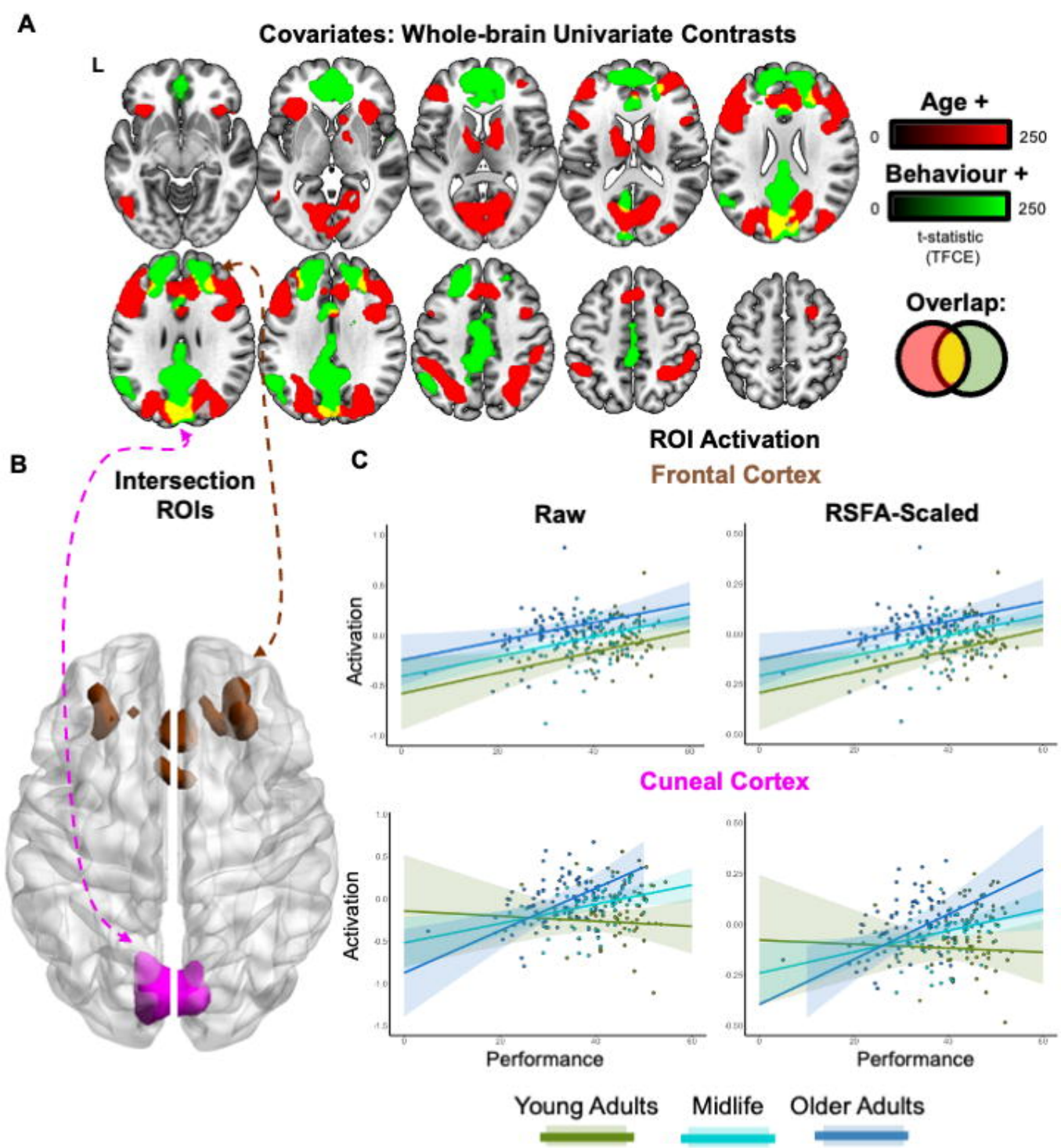
A
Covariates: Whole-brain Univariate Contrasts
L
Age +
0
250
Behaviour +
0
250
t-statistic
(TFCE)
Overlap:
B
Intersection
ROIs
ROI Activation
C
Frontal Cortex
Raw
RSFA-Scaled
Activation
Cuneal Cortex
Activation
Performance
Performance
Young Adults
Midlife
Older Adults

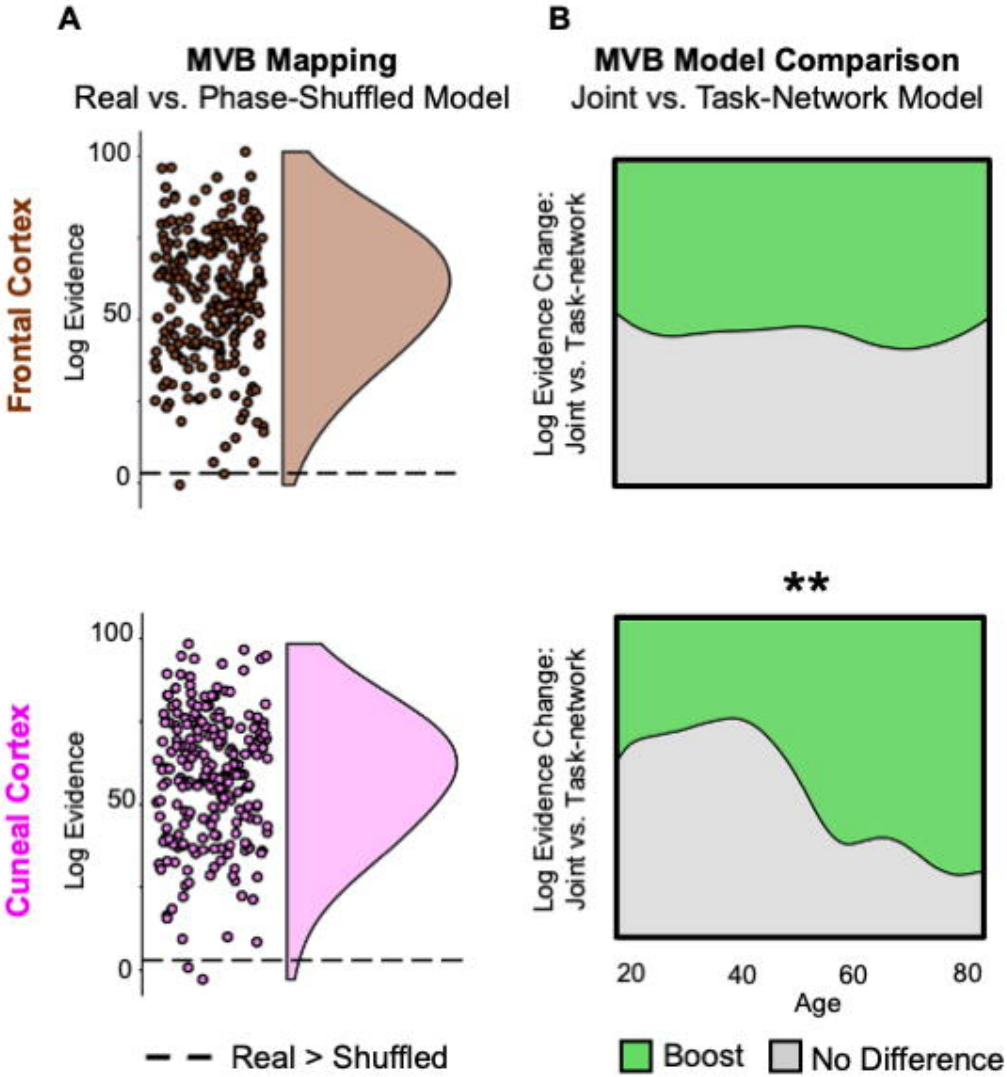
A
MVB Mapping
Real vs. Phase-Shuffled Model
B
MVB Model Comparison
Joint vs. Task-Network Model
Frontal Cortex
Cuneal Cortex
Log Evidence
100
50
0
Log Evidence Change:
Joint vs. Task-network
**
20
40
60
80
Age
Real > Shuffled
Boost
No Difference